ORIGINAL RESEARCH

Changes in Gut Microbiota and Metabolites in Papillary Thyroid Carcinoma Patients Following Radioactive Iodine Therapy

Wanting Li[1,]*, Feng Cheng[1,]*, Jun Zhang[1], Caihong Li[2], Daijing Yu[1], Halimureti Simayijiang[1], Haiyan Liu[2], Sijin Li[2], Jiangwei Yan[1]

[1]Shanxi Key Laboratory of Forensic Medicine, Shanxi Medical University, Jinzhong, People's Republic of China; [2]Department of Nuclear Medicine, First Hospital of Shanxi Medical University, Taiyuan, People's Republic of China

*These authors contributed equally to this work

Correspondence: Jiangwei Yan; Sijin Li, Tel +86 03513985386; +86 03514639352, Email yanjw@sxmu.edu.cn; lisjnm123@163.com

Purpose: Radioactive iodine therapy is administered through oral route, which is accumulated and absorbed in the intestine. However, its effects on the intestine remain unclear. In this study, we investigated the changes in the gut microbiota and metabolites following radioactive iodine therapy.

Patients and Methods: A total of 76 stool samples from the same 38 patients were collected at the start of radioactive iodine therapy and three days following the therapy. Stool microbiota and metabolites were detected using 16S rRNA gene sequencing and liquid chromatography-mass spectrometry.

Results: *Enterobacteriales, Enterobacteriaceae* and *Escherichia-Shigella* were elevated in most patients (27/38) following the therapy. The levels of 2-hydroxyundec-7-enoylcarnitine were significantly lower, whereas those of 5-dehydroavenasterol, butylisopropylamine, and salsoline-1-carboxylate were higher following the therapy. The relative abundance of *Escherichia-Shigella* was negatively correlated with 2-hydroxyundec-7-enoylcarnitine level ($r^2 = -0.661$, $P = 0.009$). Functional pathways were predicted to be involved in amino acid and lipid metabolism following the therapy. Particularly, phenylalanine, linoleic acid, sphingolipid, purine, and alpha-linolenic acid metabolism were the main metabolic pathways.

Conclusion: Gut microbiota was disturbed following radioactive iodine therapy, with increased *Escherichia-Shigella*. Processes associated with energy production seems to be impacted following the therapy, with significantly decreased 2-hydroxyundec-7-enoylcarnitine level. Meanwhile, some metabolites and functional pathways may have a positive effect on intestinal homeostasis, and may be related to the repair and promotion of gut recovery following the therapy. This study provides a basic foundation to explore how radioactive iodine affects gut microbiota and metabolites, and how gut function is regulated in response to radioactive iodine therapy.

Keywords: radioactive iodine, gut microbiota, *Escherichia-Shigella*, metabolism, thyroid carcinoma

Introduction

Thyroid carcinoma was ranked as the fifth common malignancy in women from cancer statistics in 2020.[1] Differentiated thyroid carcinomas approximately account for 90% of all types of thyroid carcinoma. Patients with differentiated thyroid carcinomas had excellent survival outcomes, mainly due to the combination of surgery and appropriate radioactive iodine therapy.[2] Radioactive iodine therapy is proposed for the ablation of remnant thyroid tissue or iodine-avid metastases.[3]

Radioactive iodine is administered through oral route, which is accumulated and absorbed in the intestine, thus it may affect the gut microbiota or metabolites. To date, few studies have reported changes in the gut microbiota or metabolites of patients with thyroid carcinoma following radioactive iodine therapy. Previous studies have indicated that gut microbiota is associated with thyroid carcinoma.[4–6] Another study investigated the dysbiosis of gut microbiota and

4453

metabolites in mice, six days following abdominal irradiation exposure.[7] In addition, gut bacterial compositions also changed in mice, seven days following total body radiation.[8]

Given the paucity of studies on the gut microbiota or metabolites in thyroid carcinoma patients following radioactive iodine therapy, we report this research.

Materials and Methods

Clinical Sample Collection

The study protocol was approved by the Ethics Committee of the First Hospital of Shanxi Medical University (K-K176), in accordance with the Declaration of Helsinki. Written informed consent was obtained from all participants. The study was conducted in the First Hospital of Shanxi Medical University from November 2020 to October 2021. Inclusion criteria included thyroid carcinoma patients (above 18 years old) preparing for radioactive iodine therapy. Participants were excluded on condition that they had been diagnosed with other diseases, such as diabetes, hypertension, coronary heart disease, or gastrointestinal disease. Exclusion factors included taking antibiotics within one month,[9] and being vegan. Stool samples were collected with swabs at the start of radioactive iodine therapy (pre-therapy) and three days following the therapy (post-therapy) and transferred using cryogenic ice to the laboratory within two hours.

DNA Extraction, Library Construction and 16S rRNA Gene Sequencing

DNA extraction was performed using the DNeasy PowerSoil Kit (Qiagen, Hilden, Germany) on the same day as sample collection and then stored at −20 °C. The V3-V4 region of the 16S rRNA gene was amplified using the primers 341F (5'-CCTACGGGNGGCWGCAG-3') and 806R (5'-GGACTACHVGGGTWTCTAAT-3'). The KOD Plus Neo PCR kit (Toyobo, Osaka, Japan) was used for the polymerase chain reaction. The size of the constructed library was determined by 2% agarose gels. Then the constructed library was purified using the Agencourt AMPure XP beads (Beckman Coulter, Miami, USA). Library quantification was performed using a QuantStudio 5 Real-Time PCR System (Applied Biosystems, California, USA). Paired-end sequencing was performed using the Miseq Reagent Kit V3 and the Illumina MiSeq instrument (Illumina, San Diego, USA).

Bioinformatics Analysis

Quality control, sequence merging and dereplication of raw reads were conducted using a combination of QIIME,[10] Cutadapt[11] and VSEARCH.[12] Samples with more than 10,000 reads were included in the subsequent analyses. Amplicon sequence variants (ASVs) were recognized using USEARCH-UNOISE3 with R (v4.1.1).[13] For each sequence of ASVs, Silva database (v132) was used to annotate the taxonomic information. STAMP (v2.1.3) and linear discriminant analysis effect size (LEfSe) were performed to determine the statistical significance of taxa.[14] Bar graphs of the microbiota at the phylum and genus levels were presented on the Tutools platform (http://www.cloudtutu.com). Spearman correlation analysis was used to visualize the relationship between differential microbiota and metabolites using GraphPad Prism (v9.3.0).

Metabolite Extraction

Metabolites were extracted using a mixed solution of 400 μL methanol:water (4:1, v/v). And 0.02 mg/mL L-2-chlorophenylalanin was used as the internal standard. The mixture was treated with tissue crusher Wonbio-96c (wanbo biotechnology, Shanghai, China) at 50 Hz for 6 min at −10 °C. The samples were set at −20 °C to precipitate proteins for 30 min after treated with ultrasound at 5 °C for 30 min at 40 kHz. The supernatant was transferred to sample vials for liquid chromatography-mass spectrometry (LC-MS) analysis after centrifugation at 13,000 × g for 15 min at 4 °C. The quality control sample was prepared by mixing equal volumes of all samples and was tested in the same way as the analytical samples.

UHPLC-MS/MS and Data Analysis

A UHPLC-Q Exactive HF-X system (Thermo Fisher Scientific, Massachusetts, USA) was used for LC-MS analysis. Raw data were processed using the Progenesis QI software (Waters Corporation, Milford, USA). False-positive peaks, including derivatized reagent peaks, column bleeds, and noise, were removed. The metabolites were identified using the Human Metabolome Database (HMDB) (http://www.hmdb.ca/). Metabolic features of detection at least 80% in all the samples were retained. Each metabolite was normalized by sum normalization method. The response intensity of the mass spectrum peaks of the samples was normalized by the sum to reduce the errors caused by instrument instability and sample preparation. Variables with a relative standard deviation > 30% of the quality control samples were removed. Partial least squares discriminant analysis (PLS-DA) was performed using R package to distinguish the pre- and post-therapy groups. Differential metabolites were selected using PLS-DA, based on variable importance in projection (VIP). Differential metabolites were mapped to biochemical pathways based on the Kyoto Encyclopedia of Genes and Genomes (KEGG) database (http://www.genome.jp/kegg/). Python packages (scipy.stats) (https://docs.scipy.org/doc/scipy/) were used to identify significantly enriched pathways following the therapy, using Fisher's exact test.

Statistical Analysis

Differences in the abundance of microbiota were assessed using Welch's t-test with Bonferroni correction. LEfSe was applied with a threshold linear discriminant analysis (LDA) score > 2.0. The differential metabolites with variable important in projection (VIP) > 1 and $P < 0.05$ were statistically significant. Differential metabolites were further identified using the Mann–Whitney U-test. A P significance was set at less than 0.05.

Results

Clinical Characteristics of the Patients

A total of 76 stool samples from the same 38 patients were collected at the start of radioactive iodine therapy (pre-therapy) and three days following the therapy (post-therapy). The study included 28 females and 10 males, with an average age of 43.473 ± 13.012 years. All the patients received radioactive iodine, 1 with 1110 MBq, 25 with 3700 MBq, 3 with 4625 MBq, 1 with 4810 MBq, 5 with 5550 MBq, 1 with 6660 MBq, and 2 with 9250 MBq. The clinical characteristics of the patients were showed in Table 1.

Table 1 Baseline Characteristics of Patients Who Received Radioactive Iodine Therapy

Baseline Characteristics	Patients (n=38)
Age (years)	43.473 ± 13.012
Female/male	28/10
BMI (kg/m^2)	25.085 ± 3.298
Maximum tumor diameter (cm)	1.392 ± 0.878
Extrathyroidal extension (yes/no)	8/30
Unilateral/bilateral focus	11/27
Multiple/single focus	12/26
Serum thyroglobulin (ng/mL)	2.205 (0.160, 15.865)
Radioactive iodine dose	
1110 MBq	1
3700 MBq	25
4625 MBq	3
4810 MBq	1
5550 MBq	5
6660 MBq	1
9250 MBq	2

Microbiota Composition in Pre-Therapy and Post-Therapy Groups and Microbial Alteration in Patients Following Radioactive Iodine Therapy

A total of 2114 ASVs were annotated into following results, kingdom, 1; phylum, 6; class,16; order, 21; family, 34; genus, 76. Microbiota profiles at the phylum and genus levels were listed in Supplementary Table 1 and Supplementary Table 2. The top four phyla were Firmicutes, Bacteroidetes, Proteobacteria, and Actinobacteria in pre-therapy group (Figure 1A). At the genus level, *Prevotella* was prominent in the pre-therapy group, followed by *Bacteroides, Finegoldia, Ezakiella, Faecalibacterium, Peptoniphilus, Campylobacter* and *Anaerococcus* (Figure 1B). Firmicutes, Bacteroidetes, Proteobacteria, and Actinobacteria were also enriched in post-therapy group (Figure 2A). *Prevotella* was prominent in the post-therapy group, followed by *Bacteroides, Faecalibacterium, Finegoldia, Ezakiella, Escherichia-Shigella, Campylobacter* and *Peptoniphilus* (Figure 2B).

LEfSe showed that *Enterobacteriales, Enterobacteriaceae* and *Escherichia-Shigella* were elevated in the post-therapy group compared with the pre-therapy group (Figure 3A). The relative abundance of *Escherichia-Shigella* was higher in the post-therapy group than in the pre-therapy group ($P = 0.010$) (Figure 3B). In addition, for each patient, the relative abundance of *Escherichia-Shigella* increased in twenty-seven patients following the therapy, and decreased in eleven patients (Figure 3C). The eleven patients received radioactive iodine, one patient with 1110 MBq, seven with 3700 MBq, one with 5550 MBq, and two with 9250 MBq.
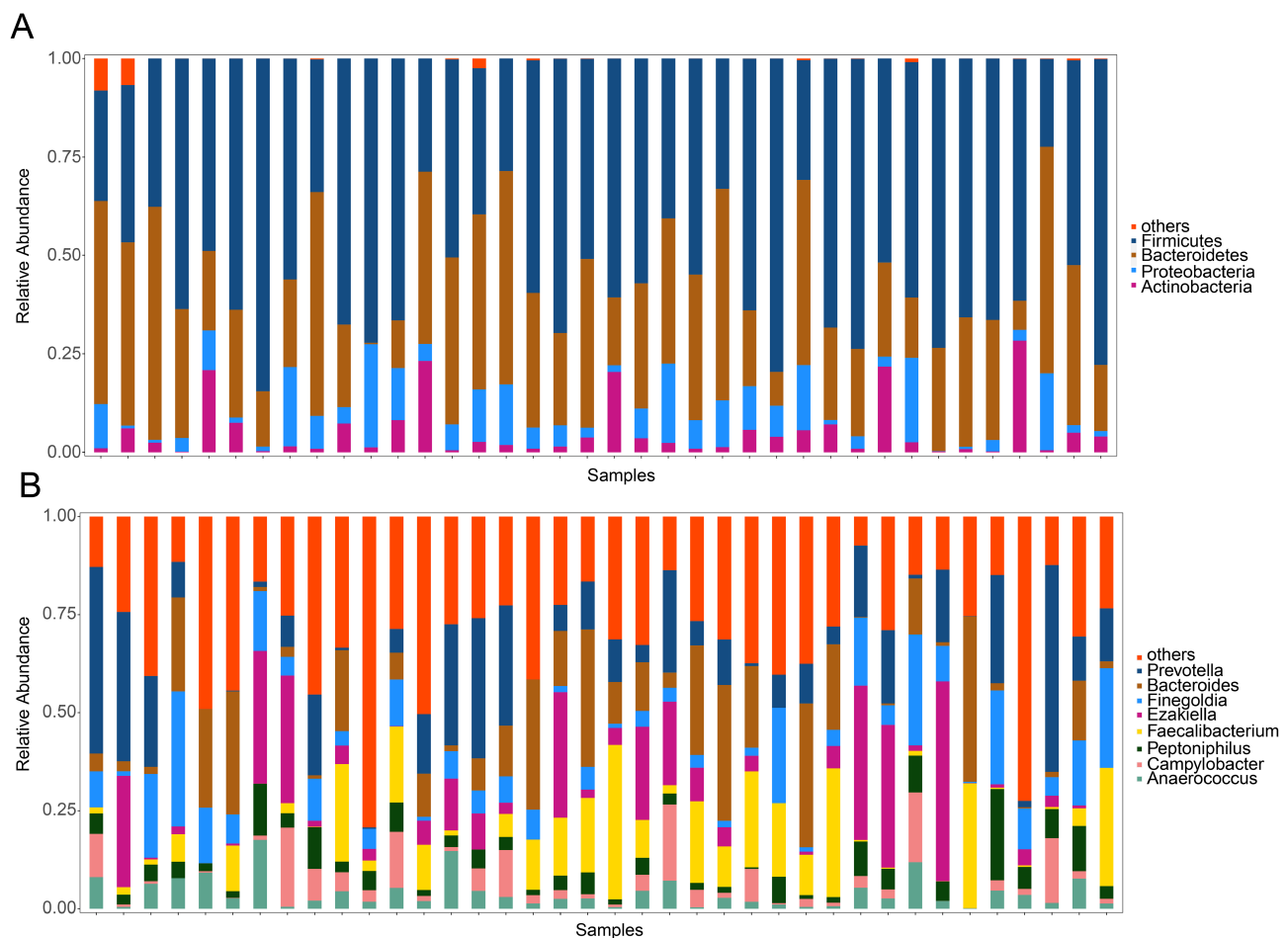

Figure 1 A bar plot of the relative abundance of gut microbial composition in patients at the start of radioactive iodine therapy.
Notes: (**A**) Top four phyla at the phylum level. (**B**)Top eight genera at the genus level. The abscissa represents different individuals. The ordinate represents the relative abundance of microbiota.

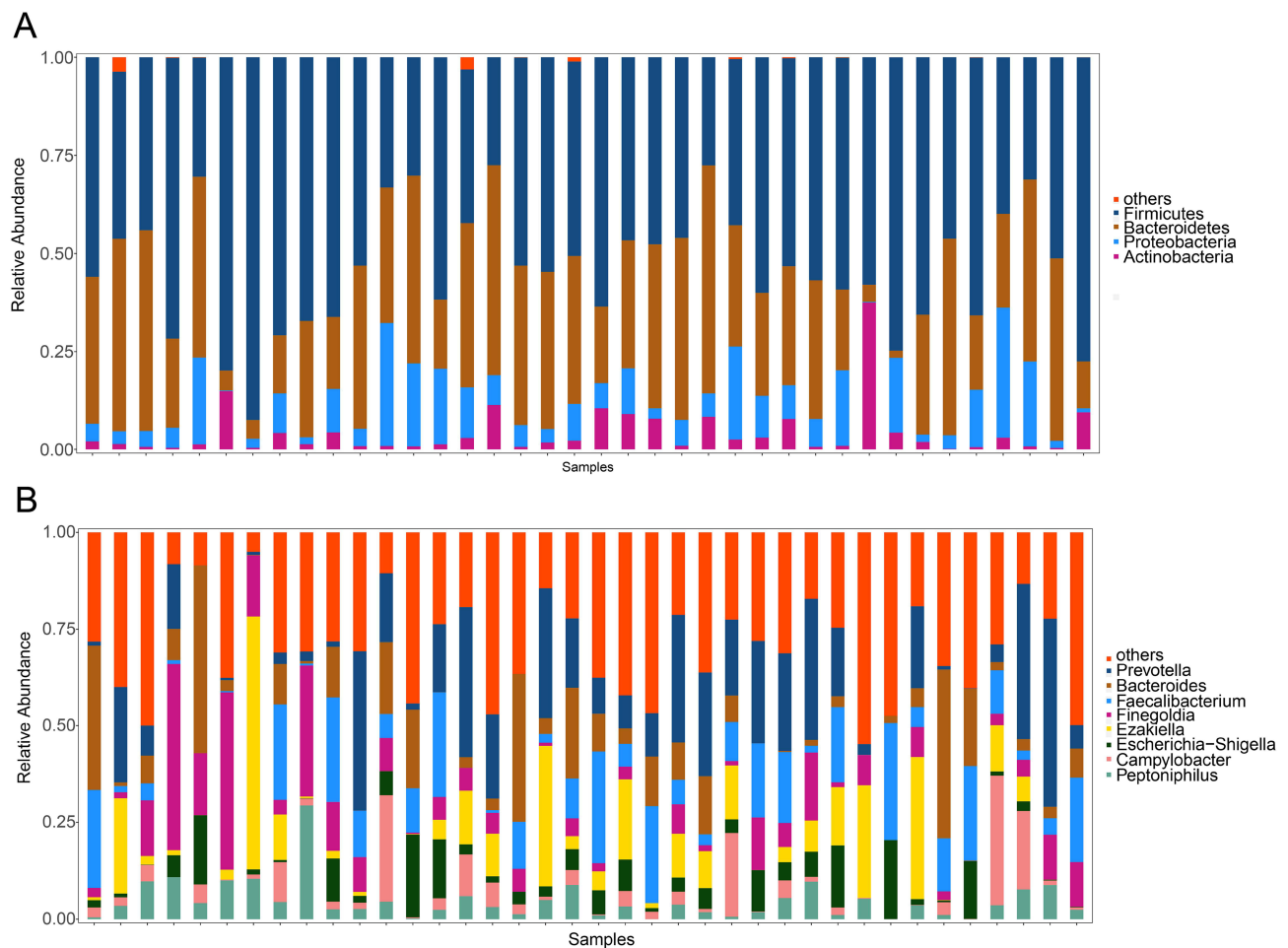**Figure 2** A bar plot of the relative abundance of gut microbial composition in patients following radioactive iodine therapy.
Notes: (**A**) Top four phyla. (**B**)Top eight genera. Different color indicates distinct microbiota at phylum and genus level.

Changes of Metabolite Profiles in Patients Following Radioactive Iodine Therapy

To further investigate metabolite profiles, 30 stool samples were detected using liquid chromatography-mass spectrometry from 15 patients of pre-therapy and post-therapy. A total of 5828 cationic ions (1602 metabolites identified) and 5588 anionic ions (1047 metabolites identified) were obtained. The compounds that matched the HMDB database were shown in Figure 4A. Lipid-related metabolites account for the largest proportion, followed by organic acids, and organoheterocyclic compounds. The pre- and post-therapy groups were separated into distinct clusters by PLS-DA score analysis, for both positive compounds (Figure 4B) and negative compounds (Figure 4C). The permutation test for PLS-DA showed that the Q^2 and R^2 values on the left were lower than those on the right (original points). In addition, the Q^2 regression line had a negative intercept, with $R^2 > 0.5$, indicating that the PLS-DA method was valid for positive compounds (Figure 4D) and negative compounds (Figure 4E).

In detail, 20 differential positive compounds and 10 negative compounds were identified (VIP > 1.0, $P < 0.05$, Figure 5A). Compared to pre-therapy group, 15 metabolites showed higher concentrations and 15 metabolites showed lower concentrations in the post-therapy group. Except for the exogenous metabolites, five differential metabolites were further selected, using the non-parametric Mann–Whitney U-test. Among them, agmatine was excluded, which was inconsistent with the sample size estimation.[15] The levels of 2-hydroxyundec-7-enoylcarnitine (Figure 5B) were significantly lower in the post-therapy group, whereas butylisopropylamine (Figure 5C), 5-dehydroavenasterol (Figure 5D) and salsoline-1-carboxylate levels (Figure 5E) were higher than those in the pre-therapy group.
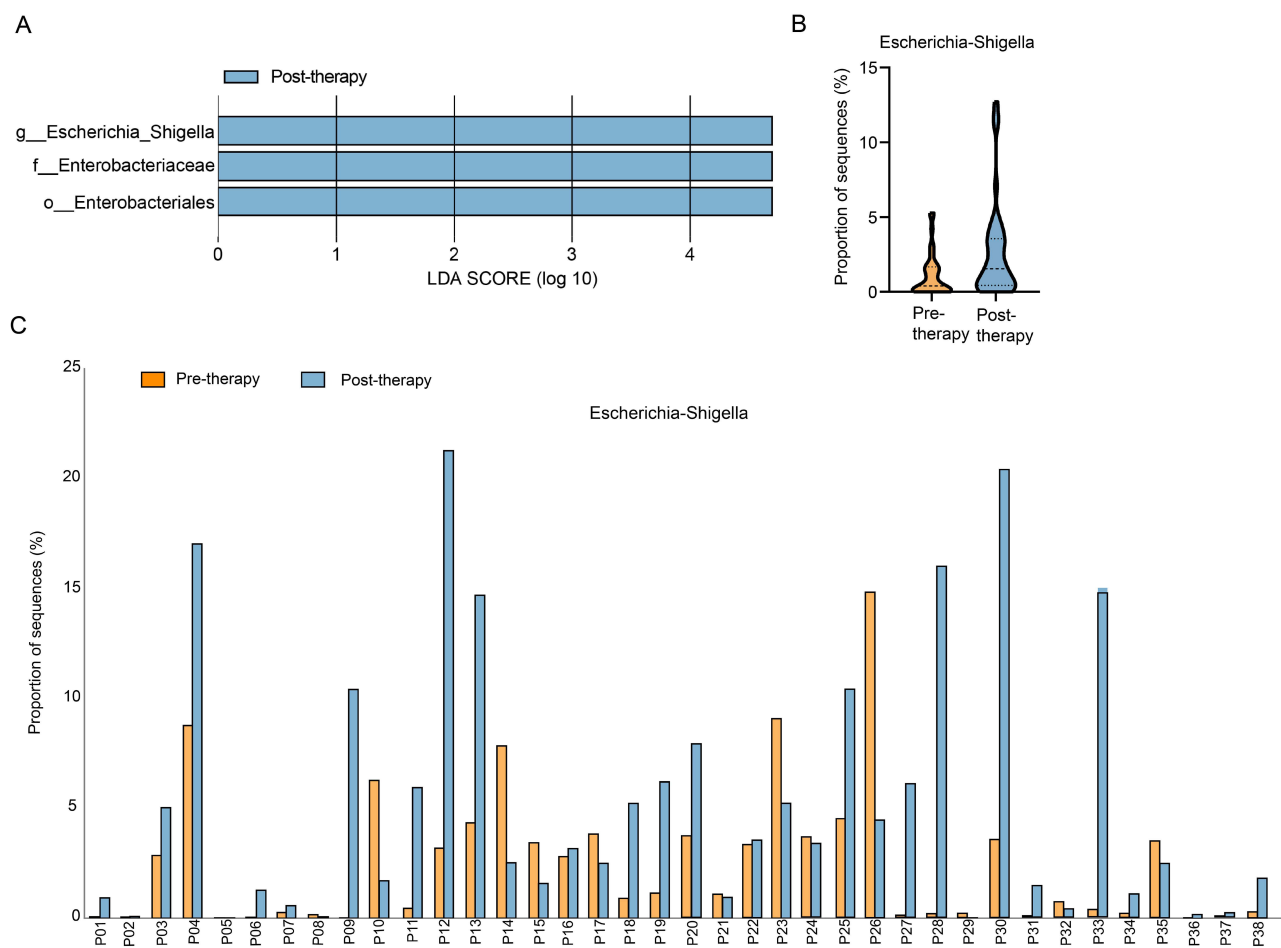
Figure 3 Change in gut microbiota of patients following radioactive iodine therapy.
Notes: (**A**) Linear discriminant analysis effect size (LEfSe) to identify the significant microbiota following radioactive iodine therapy. Taxa meeting a linear discriminant analysis (LDA) threshold value > 2.0 and P < 0.05 are shown. (**B**) Violin plot of the relative abundance of *Escherichia-Shigella* in the pre- and post-therapy groups using Mann–Whitney U-test (P = 0.010). (**C**) Bar plot of the relative abundance of *Escherichia-Shigella* in each patient of pre-therapy and post-therapy.

KEGG Annotation and Enrichment of Function Pathway in Patients Following Radioactive Iodine Therapy

Three nucleic acids and one fatty acid compounds were identified using KEGG annotation (Figure 6A). The pathway classification results showed that the number of compounds involved in amino acid and lipid metabolism was higher (Figure 6B). KEGG topology analysis revealed enrichment of pathways following the therapy. Particularly, phenylalanine, linoleic acid, sphingolipid, purine and alpha-linolenic acid metabolism were the main metabolic pathways (P < 0.05, Figure 6C).

Associations Between Differential Microbiota and Metabolites

Spearman correlation analysis was used to investigate the relationship between the differential microbiota and metabolites. The relative abundance of *Escherichia-Shigella* was negatively correlated with 2-hydroxyundec-7-enoylcarnitine levels in the post-therapy group ($r^2 = -0.661$, $P = 0.009$) (Figure 7).

Discussion

To our knowledge, this is the first preliminary study to investigate early alterations in the gut microbiota and metabolites in papillary thyroid carcinoma following radioactive iodine therapy.

In this study, stool *Escherichia-Shigella* showed a mixed response to radioactive iodine, with an enrichment in most patients following radioactive iodine. *Escherichia-Shigella*, belong to Proteobacteria, which was also found to elevate
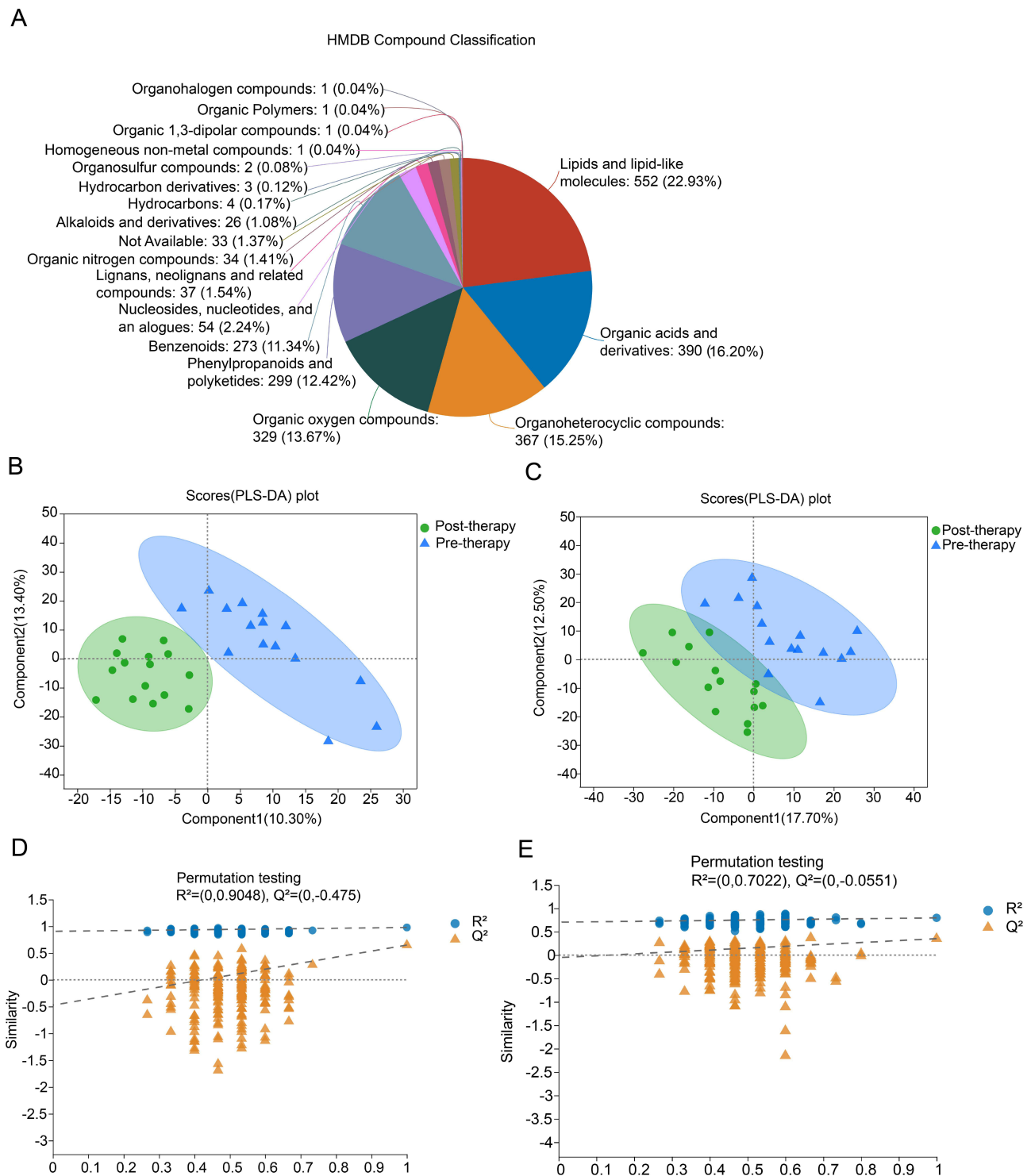
A

HMDB Compound Classification

B

C

D

E

Figure 4 Changes in metabolite profiles following radioactive iodine therapy.
Notes: (**A**) Total compounds matched the Human Metabolome Database (HMDB) in the pre- and post-therapy groups. (**B**) Pre- and post-therapy groups were separated by partial least squares discriminant analysis (PLS-DA) score analysis for positive component. (**C**) Pre- and post-therapy groups were separated by PLS-DA score analysis for negative components. (**D**) Permutation test for positive components. (**E**) Permutation test for negative components.

with radiopharmaceuticals using an ex-vivo approach in a previous study.[16] An abundance of Proteobacteria and *Escherichia-Shigella* clusters may represent an unstable gut microbial community,[17] and have been known as pathogenic microorganisms[18] in acute inflammation or human colitis-associated colorectal carcinoma.[19,20] In addition, *Escherichia-*
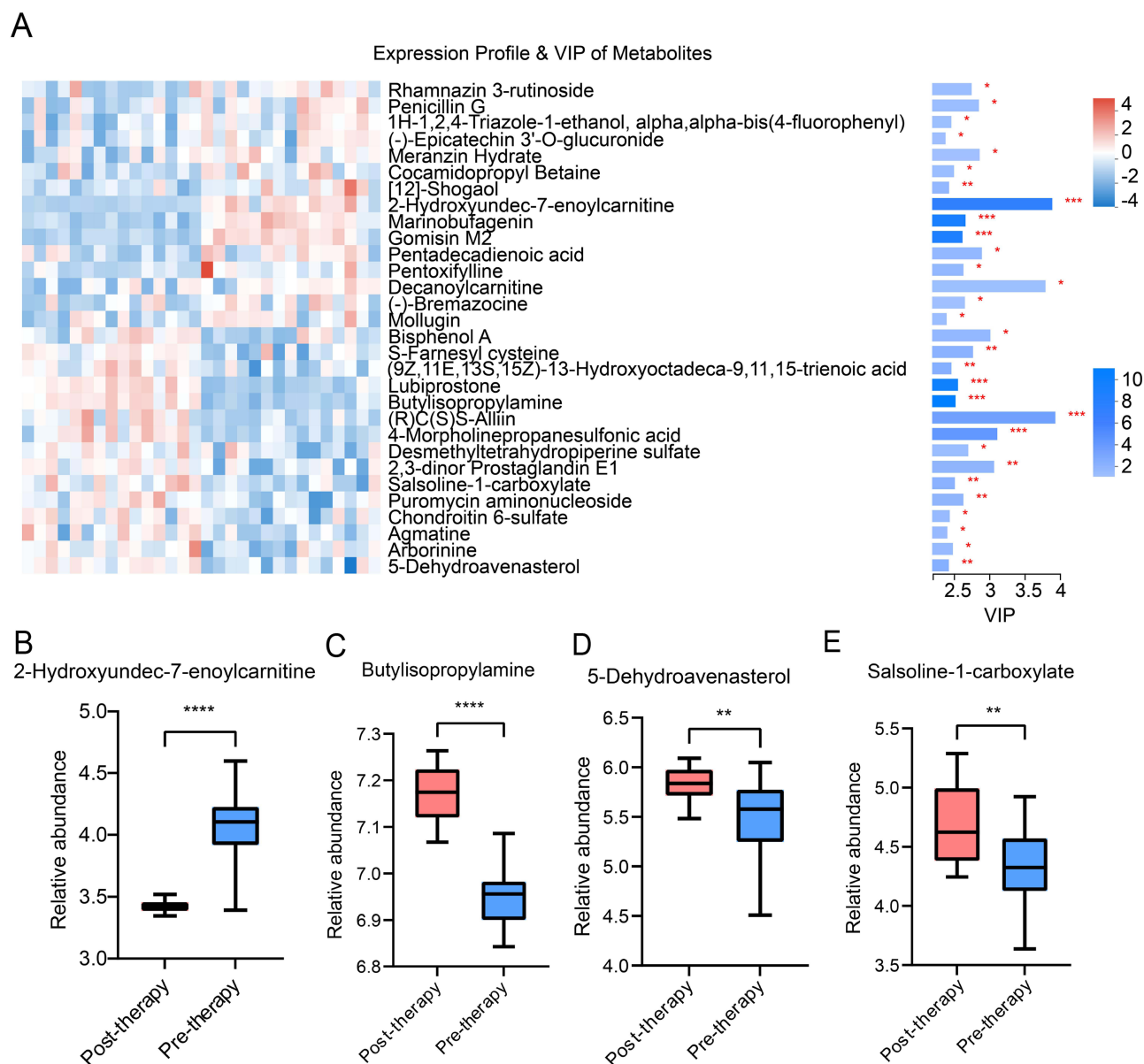
A

Expression Profile & VIP of Metabolites

Figure 5 Differential metabolite profiles following radioactive iodine therapy.
Notes: (**A**) Expression profile and variable importance in projection (VIP) score of differential metabolites. The left plot represents the expression of differential metabolites. The right plot indicates VIP score of differential metabolites, VIP > 1.0, $P < 0.05$. (**B**) The relative abundance of 2-hydroxyundec-7-enoylcarnitine. (**C**) The relative abundance of butylisopropylamine. (**D**) The relative abundance of 5-dehydroavenasterol. (**E**) The relative abundance of salsoline-1-carboxylate. Differential metabolites between pre-therapy and post-therapy groups were further identified using the Mann–Whitney U-test. *$P < 0.05$, **$P < 0.01$, ***$P < 0.001$, ****$P < 0.0001$.

Shigella is Shiga toxin-producing bacteria that may associate with DNA damage.[5] The relative abundances of *Escherichia-Shigella* showed linear correlations with radiation dose in a mouse model.[21] *Escherichia-Shigella* showed an increase in most patients in the study, that may imply the early gut microbial imbalance and dysbacteriosis following radioactive iodine therapy.

In addition to microbiota, metabolites, in the context of radioactive iodine, have also been investigated. 2-hydroxyundec-7-enoylcarnitine is an acylcarnitine that has a protective effect on the gut barrier.[22] Acylcarnitine plays a role in maintaining cell viability, restoring activities, and protecting membrane permeability.[23,24] The vital role of acylcarnitine is beta-oxidation to produce energy, transporting fatty acids and organic acids from the cytoplasm to the mitochondria. Then they can be broken down to produce energy.[25] Radiation could damage beta-oxidation and induce lipid accumulation, resulting in decreased ATP production.[26] The level of acylcarnitine in urine decreased at 6 h post-exposure to
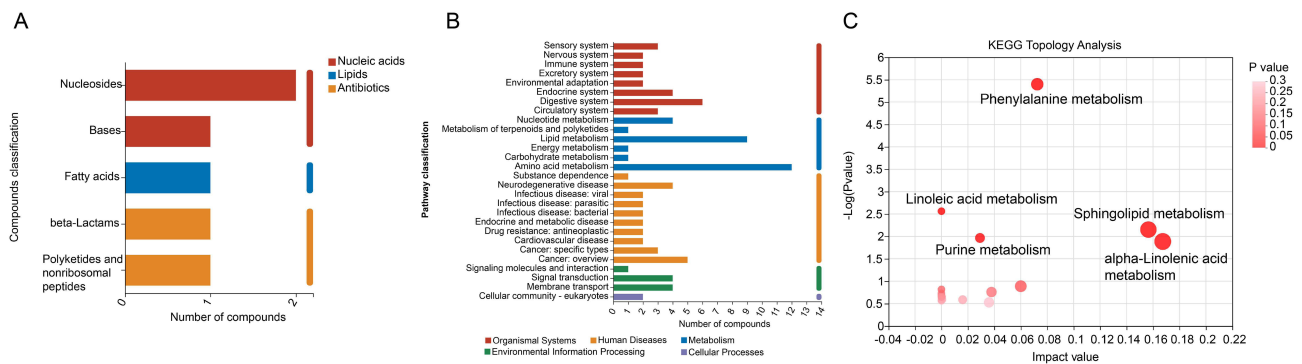
Figure 6 Predicted function pathway in patients following radioactive iodine therapy.
Notes: (**A**) Compound classification were identified using Kyoto Encyclopedia of Genes and Genomes (KEGG) annotation. (**B**) Pathway classification were identified using KEGG annotation. (**C**) KEGG topology analysis of significant pathways, and pathways meeting an $P < 0.05$ are shown.
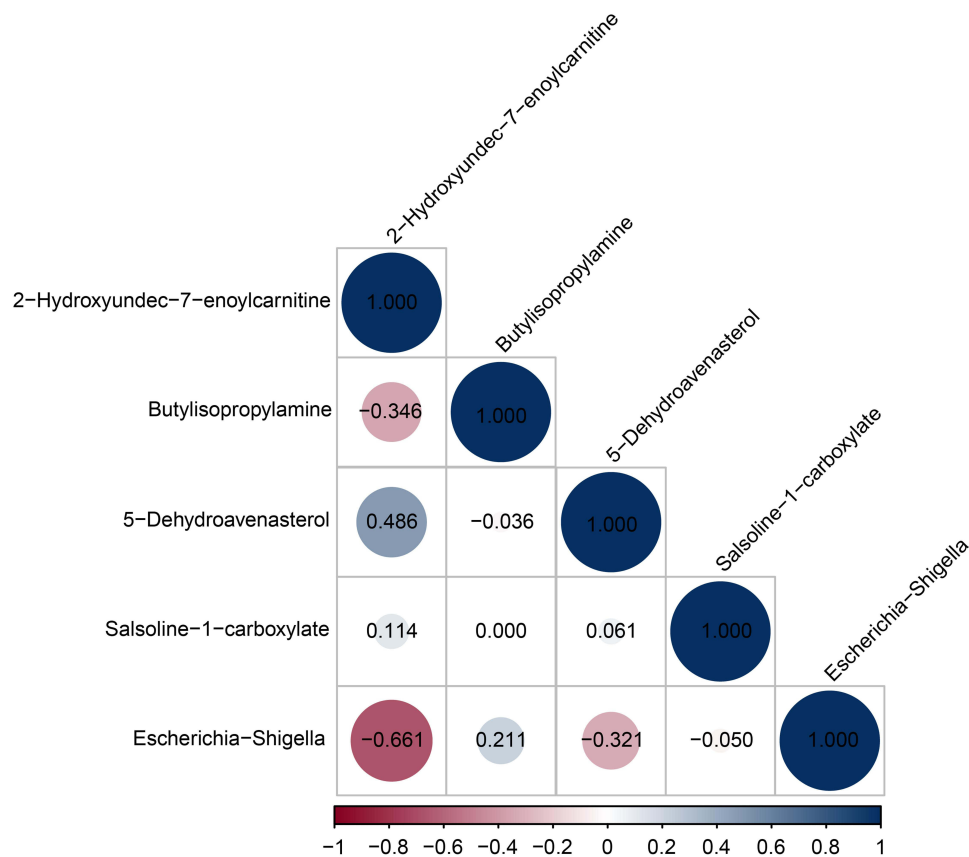

Figure 7 Heatmap correlation analysis between differential microbiota and metabolites.
Notes: The abscissa indicates correlation coefficients. The ordinate indicates differential microbiota and metabolites. The numerical value in the circles represent the correlation coefficient. Red and blue represent negative and positive correlation, respectively.

radiation in patients undergoing total body irradiation.[27] In this study, the level of 2-hydroxyundec-7-enoylcarnitine significantly decreased following the therapy. The processes associated with energy production seem to be affected following radioactive iodine therapy.

Moreover, 5-dehydroavenasterol belongs to sterol lipid, that had properties of exerting antioxidative, anti-inflammatory, and improving metabolism.[28] Salsoline-1-carboxylic is an intermediate metabolite in the process of salsoline synthesis, which has a biological activity of anti-inflammatory.[29] Alterations of these metabolites may have a positive effect on intestinal homeostasis following radioactive iodine therapy.

Next, metabolites were predicted to involve in pathways, such as phenylalanine, linoleic acid, alpha linolenic acid, and sphingolipid metabolism. Acute radiation induces inflammation of the intestinal epithelium and influences the absorption and metabolism of amino acids in mucosal epithelial cells.[30] A previous study demonstrated that phenylalanine metabolism could improve the activity of intestinal alkaline phosphatase and play a positive role in intestinal barrier function.[31] In addition, gut linoleic acid and alpha linolenic acid metabolism pathways were found to be involved in anti-inflammatory and antioxidative effects.[32,33] Sphingolipid metabolism has been implicated in gut immune reactions and is mediated by extracorporeal and intracorporeal factors.[34] The enrichment of pathways, related to phenylalanine metabolism, linoleic acid, alpha linolenic acid and sphingolipid metabolism in the study, may imply a role in repairing and promoting gut recovery following radioactive iodine therapy, worthy of further exploration.

This study has some limitations. First, it was based on single-center data with a limited sample size and single time point. A multicenter study should be further conducted. A time series with a longer follow-up will be adopted to investigate the dynamic changes in the microbiota and metabolites in the future. Second, the present work was a preliminary investigation without evidence of the mechanisms of the response to radioactive iodine, so it was impossible to determine the causal relationship between gut microbiota and metabolites. In addition, other factors should be considered, such as diet, region and stress which may affect gut microbiota composition. Despite the above limitations, this study provides a basic foundation for exploring alterations in the gut microbiota and metabolites in response to radioactive iodine therapy.

Conclusion

In summary, our study for the first time investigated the early changes in gut microbiota and metabolites following radioactive iodine therapy. *Escherichia-Shigella* increased in most patients following the therapy, with significantly decreased 2-hydroxyundec-7-enoylcarnitine and elevated 5-dehydroavenasterol, butylisopropylamine, and salsoline-1-carboxylate levels. Some metabolites and functional pathways were involved in phenylalanine metabolism, linoleic acid, alpha linolenic acid, and sphingolipid metabolism, which might be related to the repair and promotion of gut recovery following the therapy, and are worthy of further exploration.

Data Sharing Statement

The raw data in the study are available in Bioproject with accession number PRJNA889594 or upon reasonable request from the corresponding author JY.

Ethics Approval and Informed Consent Statement

The study protocol was approved by the Ethics Committee of the First Hospital of Shanxi Medical University (approval number: K-K176) in accordance with the guidelines of the World Medical Association and the Declaration of Helsinki. Written informed consent was obtained from all participants.

Acknowledgments

Author Contributions

All authors made a significant contribution to the work reported, whether that is in the conception, study design, execution, acquisition of data, analysis and interpretation, or in all these areas; all authors took part in drafting, revising or critically reviewing the article; all authors gave final approval of the version to be published; all authors have agreed on the journal to which the article has been submitted and agree to be accountable for all aspects of the work.

Funding

Disclosure

The authors report no conflicts of interest in this work.

References

1. Siegel RL, Miller KD, Jemal A. Cancer statistics, 2020. *CA Cancer J Clin*. 2020;70(1):7–30. doi:10.3322/caac.21590
2. Tuttle RM, Ahuja S, Avram AM, et al. Controversies, Consensus, and Collaboration in the Use of (131) I Therapy in Differentiated Thyroid Cancer: a Joint Statement from the American Thyroid Association, the European Association of Nuclear Medicine, the Society of Nuclear Medicine and Molecular Imaging, and the European Thyroid Association. *Thyroid*. 2019;29(4):461–470. doi:10.1089/thy.2018.0597
3. Schlumberger M, Leboulleux S. Current practice in patients with differentiated thyroid cancer. *Nat Rev Endocrinol*. 2021;17(3):176–188. doi:10.1038/s41574-020-00448-z
4. Yu X, Jiang W, Kosik RO, et al. Gut microbiota changes and its potential relations with thyroid carcinoma. *J Adv Res*. 2022;35:61–70. doi:10.1016/j.jare.2021.04.001
5. Feng J, Zhao F, Sun J, et al. Alterations in the gut microbiota and metabolite profiles of thyroid carcinoma patients. *Int J Cancer*. 2019;144 (11):2728–2745. doi:10.1002/ijc.32007
6. Lu G, Yu X, Jiang W, et al. Alterations of Gut Microbiome and Metabolite Profiles Associated with Anabatic Lipid Dysmetabolism in Thyroid Cancer. *Front Endocrinol (Lausanne)*. 2022;13:893164. doi:10.3389/fendo.2022.893164
7. Xiao HW, Cui M, Li Y, et al. Gut microbiota-derived indole 3-propionic acid protects against radiation toxicity via retaining acyl-CoA-binding protein. *Microbiome*. 2020;8(1):69. doi:10.1186/s40168-020-00845-6
8. Guo H, Chou WC, Lai Y, et al. Multi-omics analyses of radiation survivors identify radioprotective microbes and metabolites. *Science*. 2020;370 (6516). doi:10.1126/science.aay9097
9. Keller MK, Brandsborg E, Holmstrøm K, Twetman S. Effect of tablets containing probiotic candidate strains on gingival inflammation and composition of the salivary microbiome: a randomised controlled trial. *Benef Microbes*. 2018;9(3):487–494. doi:10.3920/bm2017.0104
10. Caporaso JG, Kuczynski J, Stombaugh J, et al. QIIME allows analysis of high-throughput community sequencing data. *Nat Methods*. 2010;7 (5):335–336. doi:10.1038/nmeth.f.303
11. Kechin A, Boyarskikh U, Kel A, Filipenko M. cutPrimers: a New Tool for Accurate Cutting of Primers from Reads of Targeted Next Generation Sequencing. *J Comput Biol*. 2017;24(11):1138–1143. doi:10.1089/cmb.2017.0096
12. Rognes T, Flouri T, Nichols B, Quince C, Mahé F. VSEARCH: a versatile open source tool for metagenomics. *PeerJ*. 2016;4:e2584. doi:10.7717/peerj.2584
13. Liu YX, Qin Y, Chen T, et al. A practical guide to amplicon and metagenomic analysis of microbiome data. *Protein Cell*. 2021;12(5):315–330. doi:10.1007/s13238-020-00724-8
14. Segata N, Izard J, Waldron L, et al. Metagenomic biomarker discovery and explanation. *Genome Biol*. 2011;12(6):R60. doi:10.1186/gb-2011-12-6-r60
15. Ceyhan C, Murat C, Doğan Y, Muhittin AS. Sample size, power and effect size revisited: simplified and practical approaches in pre-clinical, clinical and laboratory studies. *Biochem Med (Zagreb)*. 2021;31(1). doi:10.11613/BM.2021.010502
16. Fernandes A, Oliveira A, Guedes C, Fernandes R, Soares R, Barata P. Ionizing Radiation from Radiopharmaceuticals and the Human Gut Microbiota: an Ex Vivo Approach. *Int J Mol Sci*. 2022;23(18). doi:10.3390/ijms231810809
17. Fei N, Zhao L. An opportunistic pathogen isolated from the gut of an obese human causes obesity in germfree mice. *Isme j*. 2013;7(4):880–884. doi:10.1038/ismej.2012.153
18. Mukhopadhya I, Hansen R, El-Omar EM, Hold GL. IBD-what role do Proteobacteria play? *Nat Rev Gastroenterol Hepatol*. 2012;9(4):219–230. doi:10.1038/nrgastro.2012.14
19. Walujkar SA, Dhotre DP, Marathe NP, Lawate PS, Bharadwaj RS, Shouche YS. Characterization of bacterial community shift in human Ulcerative Colitis patients revealed by Illumina based 16S rRNA gene amplicon sequencing. *Gut Pathog*. 2014;6:22. doi:10.1186/1757-4749-6-22
20. Gevers D, Kugathasan S, Denson LA, et al. The treatment-naive microbiome in new-onset Crohn's disease. *Cell Host Microbe*. 2014;15 (3):382–392. doi:10.1016/j.chom.2014.02.005
21. Zhao TS, Xie LW, Cai S, et al. Dysbiosis of Gut Microbiota Is Associated With the Progression of Radiation-Induced Intestinal Injury and Is Alleviated by Oral Compound Probiotics in Mouse Model. *Front Cell Infect Microbiol*. 2021;11:717636. doi:10.3389/fcimb.2021.717636
22. Zhou R, He D, Xie J, et al. The Synergistic Effects of Polysaccharides and Ginsenosides from American Ginseng (Panax quinquefolius L.) Ameliorating Cyclophosphamide-Induced Intestinal Immune Disorders and Gut Barrier Dysfunctions Based on Microbiome-Metabolomics Analysis. *Front Immunol*. 2021;12:665901. doi:10.3389/fimmu.2021.665901
23. Marcovina SM, Sirtori C, Peracino A, et al. Translating the basic knowledge of mitochondrial functions to metabolic therapy: role of L-carnitine. *Transl Res*. 2013;161(2):73–84. doi:10.1016/j.trsl.2012.10.006
24. Mansour HH. Protective role of carnitine ester against radiation-induced oxidative stress in rats. *Pharmacol Res*. 2006;54(3):165–171. doi:10.1016/j.phrs.2006.04.003
25. Dambrova M, Makrecka-Kuka M, Kuka J, et al. Acylcarnitines: nomenclature, Biomarkers, Therapeutic Potential, Drug Targets, and Clinical Trials. *Pharmacol Rev*. 2022;74(3):506–551. doi:10.1124/pharmrev.121.000408
26. Tan Z, Xiao L, Tang M, et al. Targeting CPT1A-mediated fatty acid oxidation sensitizes nasopharyngeal carcinoma to radiation therapy. *Theranostics*. 2018;8(9):2329–2347. doi:10.7150/thno.21451
27. Laiakis EC, Mak TD, Anizan S, et al. Development of a metabolomic radiation signature in urine from patients undergoing total body irradiation. *Radiat Res*. 2014;181(4):350–361. doi:10.1667/rr13567.1
28. Wen S, He L, Zhong Z, et al. Stigmasterol Restores the Balance of Treg/Th17 Cells by Activating the Butyrate-PPARγ Axis in Colitis. *Front Immunol*. 2021;12:741934. doi:10.3389/fimmu.2021.741934
29. Ibrayev MK, Nurkenov OA, Rakhimberlinova ZB, et al. Synthesis, Structure and Molecular Docking of New 4,5-Dihydrothiazole Derivatives Based on 3,5-Dimethylpyrazole and Cytisine and Salsoline Alkaloids. *Molecules*. 2022;27(21). doi:10.3390/molecules27217598

30. Li Y, Sui L, Zhao H, et al. Differences in the Establishment of Gut Microbiota and Metabolome Characteristics Between Balb/c and C57BL/6J Mice After Proton Irradiation. *Front Microbiol*. 2022;13:874702. doi:10.3389/fmicb.2022.874702

31. Chen L, Yang P, Hu L, Yang L, Chu H, Hou X. Modulating phenylalanine metabolism by L. acidophilus alleviates alcohol-related liver disease through enhancing intestinal barrier function. *Cell Biosci*. 2023;13(1):24. doi:10.1186/s13578-023-00974-z

32. Zhao J, Cheng W, Lu H, et al. High fiber diet attenuate the inflammation and adverse remodeling of myocardial infarction via modulation of gut microbiota and metabolites. *Front Microbiol*. 2022;13:1046912. doi:10.3389/fmicb.2022.1046912

33. Gao X, Chang S, Liu S, et al. Correlations between α-Linolenic Acid-Improved Multitissue Homeostasis and Gut Microbiota in Mice Fed a High-Fat Diet. *mSystems*. 2020;5(6). doi:10.1128/mSystems.00391-20

34. Kunisawa J, Kiyono H. Sphingolipids and Epoxidized Lipid Metabolites in the Control of Gut Immunosurveillance and Allergy. *Front Nutr*. 2016;3:3. doi:10.3389/fnut.2016.00003